БЪЛГАРСКА АКАДЕМИЯ НА НАУКИТЕ • BULGARIAN ACADEMY OF SCIENCES

ГЕОХИМИЯ, МИНЕРАЛОГИЯ И ПЕТРОЛОГИЯ • 42 • СОФИЯ • 2005
GEOCHEMISTRY, MINERALOGY AND PETROLOGY • 42 • SOFIA • 2005

Volcanology and petrology of acid volcanic rocks from the Paleogene Sheinovets caldera, Eastern Rhodopes

Rositsa Ivanova

Abstract. The Sheinovets caldera is an integral part of the Maritsa group volcanoes located in the northeasternmost portion of the Eastern Rhodopes Paleogene volcanic area. A fragment of the caldera presently constitutes the easternmost part of the Ibredjeck horst where a thick sequence of sedimentary and volcaniclastic rocks is exposed. High-K rhyolite domes and dykes are also present. The tuffs are massive, poorly sorted and contain lithics (both pumice and dense lava), crystal clasts and glass shards. They were probably deposited from dense pyroclastic flows generated by high plinian column collapse. The topmost parts of the section comprise lithic-rich pyroclastic breccias, resulting from block and ash flows formed during the emplacement and growth of lava domes through directed blasts, explosive or gravitational dome collapse.

On the base of their K-Ar age, the rhyolite bodies are divided into two groups: Malko-Gradishte (Priabonian) and Sheinovets (Rupelian). The rhyolites from both groups are high-K and scarcely porphyritic. The phenocryst assemblages consist of plagioclase and biotite (± sanidine, quartz, amphibole, pyroxene). Calculated temperature of two-feldspar crystallization is slightly below 700°C. Estimated pressure of amphibole+plagioclase crystallization is about 2 kbar corresponding to depths of 6-7 km. The geochemical features of the rhyolites can be attributed to plagioclase-dominated fractional crystallization with participation of amphibole, biotite and accessory minerals. The high uniformity of lava pyroclasts and their resemblance to rhyolites from domes and dykes are indicative of a long-lived and significantly homogenized magma chamber that had fed all Maritsa group acid volcanoes. Existing gradients in the volatile content, crystal assemblage and degree of contamination by more mafic magma can be supposed on the base of variations in phenocrysts chemistry and their associations in the eruptive products.

Key words: acid pyroclastics, high-K rhyolites, Paleogene volcanism, Eastern Rhodopes
Address: Geological Institute, Bulgarian Academy of Sciences, 1113 Sofia, Bulgaria; E-mail: rossiv@geology.bas.bg

Иванова, Р. 2005. Петрология на киселите вулкански скали от палеогенската калдера Шейновец, Източни Родопи. *Геохим., минерал. и петрол.*, **42**, 23-45.

Резюме. Калдерата Шейновец е част от Маришката група вулкани, разположена в най-североизточните части на Източнородопската палеогенска вулканска област. Част от калдерата сега изгражда най-източния участък от Ибреждекския хорст, където се разкрива дебела последователност от седиментни и вулканокластични скали, риолитови куполи и дайки. Туфите са масивни, зле сортирани. Изградени са от литокласти (пемзови и лавови), кристалокласти и стъклени фрагменти. Предполага се, че са отложени от плътни пирокластични потоци, възникнали при срутване на плиниански еруптивен стълб. Богати на литокласти пирокластични брекчи изграждат най-горните части на разреза. Те са отложени от потоци блокове и пепел, възникнали вследствие на насочени взривове в резултат на експлозивно или гравитационно разрушаване на риолитови куполи.

Въз основа на тяхната K-Ar възраст риолитовите тела са обособени в две групи: Малкоградищенска (приабон) и Шейновецка (рупел). Риолитите и от двете групи са високо-К и бедни на порфири. Порфирните асоциации включват плагиоклаз и биотит (± санидин, кварц, амфибол, пироксен). Изчислената температура на кристализация на плагиоклаз и санидин е малко под 700°C.

Налягането, при което кристализира асоциацията амфибол+плагиоклаз, е оценено на около 2 kbar, отговарящо на дълбочина приблизително 6-7 km. Геохимичните особености на риолитите могат да се обяснят с доминирана от плагиоклаз фракционна кристализация, с възможно участие на амфибол, биотит и акцесорни минерали. Еднообразието в особеностите на лавовите пирокласти и сходството им с риолитите от куполите и дайките е указание за съществуването на една дълговивуща и в значителна степен хомогенизирана магмена камера, подхранвала всички кисели вулкани от Маришката група. Съществуването на градиенти в съдържанието на флуиди, асоциациите от кристали и степента на смесване с по-базична магма е предположено въз основа на регистрираните в еруптивните продукти изменения в състава на порфирите и техните асоциации.

Introduction

Sheinovets caldera is a structure of the Maritsa group of volcanoes located in the north-easternmost parts of the Eastern Rhodopes Paleogene volcanic area (Yanev et al., 1983). It is situated to the south of Malko-Gradishte and Mezek Village, about 10 km southwest of the town of Svilengrad.

The caldera is also known as Malko Gradishte volcano (Ivanov, 1960), Valche-Pole (Yanev et al., 1983) or Sheinovets dome-cluster, emplaced within a caldera of the same name (Yanev, 1995; 1998). Only a portion of this Paleogene volcanic structure is presently exposed in the Ibredjeck horst while other parts must have been buried beneath younger sediments around the horst.

No detailed studies of Sheinovets caldera volcanic rocks have been published except for some papers dealing with zeolitization of pyroclastics in the area (Tzvetanov et al., 1983; Aleksiev and Djourova, 1995; Aleksiev et al., 2000; Ivanova et al., 2001), our works on the stratigragraphy of the intracaldera section (Ivanova et al., 2000) and K-Ar dating of some lava bodies (Ivanova et al., 2001). The main purpose of the present paper is to fill this gap in our knowledge about Paleogene volcanics in the Eastern Rhodopes and to provide new data on the petrography and chemistry of the caldera volcanics.

Regional geology and stratigraphy

The Maritsa volcanic group includes the north-easternmost occurrences of the Paleogene volcanic rocks, which are assigned to the Momchilgrad-Arda volcanic region (Yanev et al., 1983). Apart from Sheinovets caldera, this group also includes the Lozen and Sveta-Marina volcanoes located immediately to the north and west of the caldera (Fig. 1). Lozen volcano is a composite volcanic edifice formed of the products of three phases (Yanev et al., 1975). Initially, rhyolite domes accompanied by tephra and numerous dykes and sills were emplaced. Later, postdating the caldera subsidence, subvolcanic rhyodacite bodies were intruded. Several small rhyolitic bodies and dykes are assigned to the third phase. Diorites of the so-called Lozen intrusion are also exposed (Boyanov et al., 1963). The K-Ar age of the three volcanic phases is 36.5, 36 and 35 Ma (Bogdanov, 1983; Lilov et al., 1987). Oligocene rhyolite bodies (32 Ma, Lilov et al., 1987) and associated pyroclastic rocks, located less than 5 km to the west of the studied area, are presently known as Sveta-Marina volcano (Yanev et al., 1975).

The Sheinovets caldera is exposed in the easternmost part of the Ibredjeck horst (Fig. 2). The latter is an over 25 km long, E-W trending structure located between Lozen and Bryagovo depressions (Boyanov et al., 1992; Kozhouk-harov et al., 1995). Neogene (Ahmatovo Formation) and Quaternary sediments are exposed to the north of the horst, within the Lozen depression, whereas rocks of the Late Oligocene-Miocene (?) Valche-Pole Molasse Formation fill the Bryagovo depression to the south. Mainly coarse-clastic Upper Eocene sedimentary rocks (breccia-conglomerate and coal-sandstone units) and Oligocene acid pyroclastics crop out within the Ibredjeck horst, to the west of the bounding faults of the preserved caldera portion. To the east, the area studied can be traced in Greece where mainly pyroclastic rocks and possibly one rhyolite

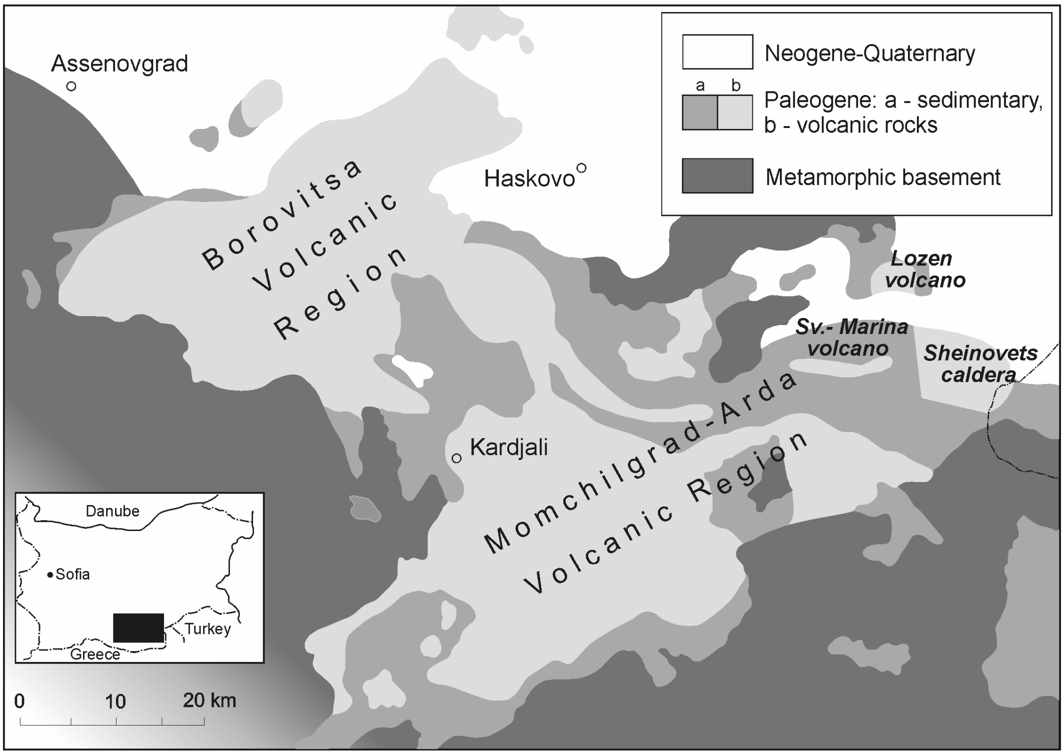

Fig. 1. Location of the Maritsa group volcanoes in the Eastern Rhodopes Paleogene volcanic area (after Yanev, 1998)
Фиг. 1. Положение на вулканите от Маришката група в Източнородопската палеогенска вулканска област (по Yanev, 1998)

body are exposed (Kirov et al., 1990; Filippidis et al., 1995; Barbiery et al., 2001).

The fill of Sheinovets caldera can be divided into two lithostratigraphic units: sedimentary and pyroclastic (Ivanova et al., 2000). The sedimentary unit forms the basal parts of the exposed section and crops out southward of the village of Malko-Gradishte. It interfingers with the lowermost exposed levels of the pyroclastic unit and underlies its upper parts. The pyroclastic unit of the intracaldera section is dominated by multiple, centimeters to tens of meters thick, non-mapable pyroclastic flow units that form an accumulation of over 1000 m in total thickness. Based on observed variations in the textural characteristics of the pyroclastic flow deposits, reflecting differences in the mode of formation, the pyroclastic unit is divided into two subunits: lower, pumice tuff packet and upper, lithic breccia packet. The pyroclastics of the lower subunit are light green, beige or pink in colour ash- and lapilli-tuffs. They are pumice-rich, massive in texture and poorly sorted. Coarse lithic-rich matrix-supported intra-flow-unit breccias are also found. The pyroclastic rocks of the upper packet are coarse-grained, lithic-rich clast-supported pyroclastic breccias.

On the base of calcareous nannofossil taxa, recorded both in sedimentary and in some epiclastic interlayers within the pyroclastic unit, the lower levels of the exposed caldera fill are assigned to the NP 21 nannofossil zone of Martini (1971), spanning the topmost part of the Priabonian and the base of the Rupelian, between 34.2 and 32.8 Ma according to data of Berggren et al. (1995) (Ivanova et al., 2000).

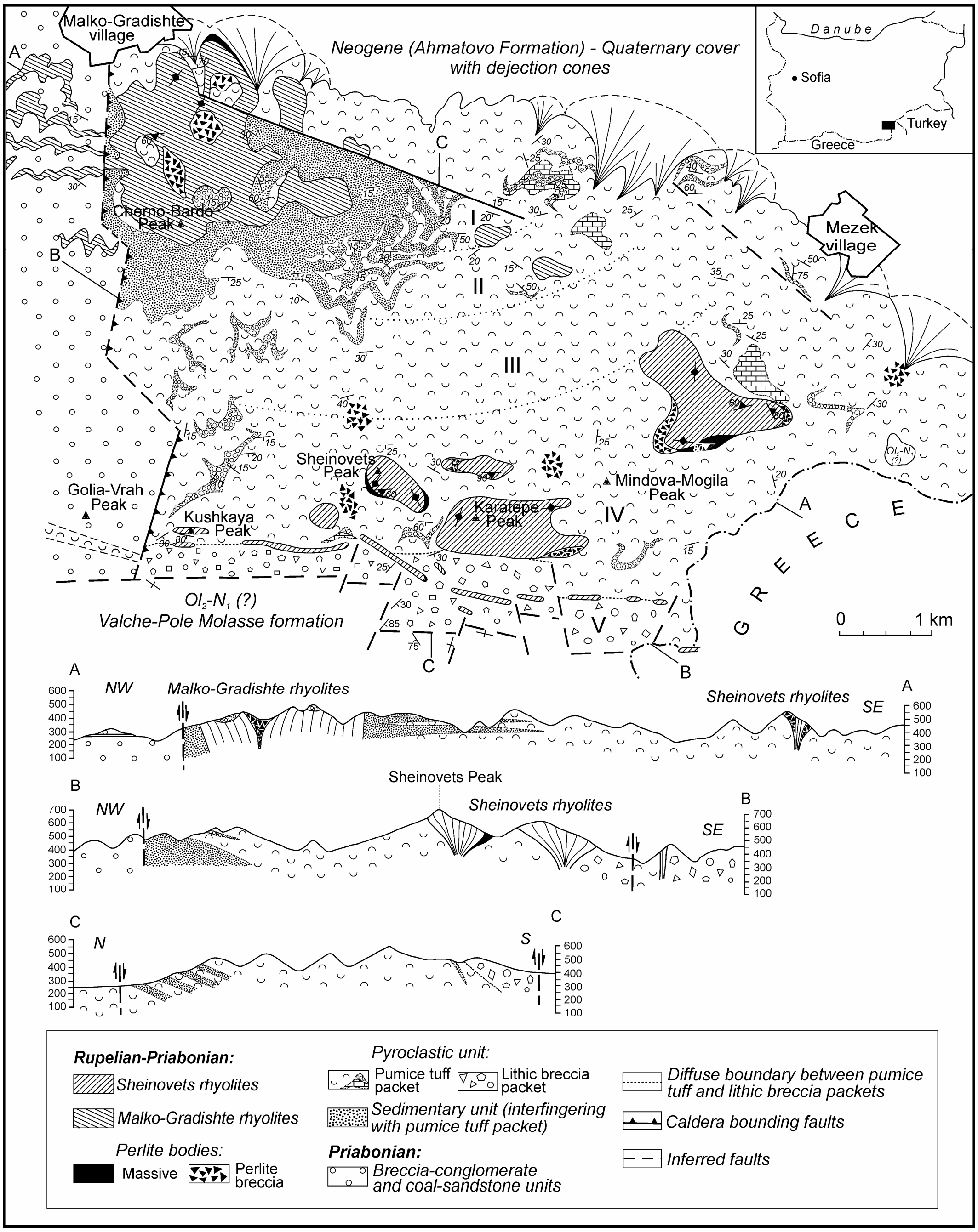

Fig. 2. Geological map of the Sheinovets caldera (modified from Ivanova et al., 2000). I-V – levels reflecting observed vertical changes in abundance and maximal size of the pyroclasts, shown in Fig. 3

Фиг. 2. Геоложка карта на Шейновецката калдера (по Ivanova et al., 2000, с допълнения). I-V – нива, отразяващи установените вертикални промени в количеството и максималния размер на пирокластите, показани на фиг. 3

Analitical techniques

Rhyolite rock powders have been prepared by removing the altered surfaces, crushing and then grounding to powder in an agate swing mill. Major and trace element abundances have been measured on fused beads (prepared of previously calcined powder fused with dehydrated $Li_2B_4O_7$ as flux and aqueous $LiBr_2$-solution as non-wetting agent on Philips Pear'x3 automatic bead machine) and pressed pellets (made of non-ignated rock powder mixed with aqueous polyvinyl alcohol solution as binder), respectively, using a sequential X-ray spectrometer Philips PW2400 at the Institute of Petrology, Vienna University. Major and some trace elements contents of six samples have been analyzed on VRA spectrometer at the X-ray fluorescence laboratory of the Geological Institute (by M. Karadjov and S. Stoyanov).

Quantitative analyses of mineral phases and silicate-melt inclusions have been performed on Cameca SX 100 electron probe microanalyser (using 15 kV acceleration voltage and 20 nA beam current) at the Institute of Petrology of Vienna University, and JEOL Superprobe 733, equipped with EDS ORTEC-5000 system, at the Geological Institute (by K. Rekalov and Tz. Iliev).

Petrographic characteristics of pyroclastic rocks

Intra-caldera pyroclastic deposits

The petrographic characteristics of the volcanoclastic part of the Sheinovets caldera fill (textural features of the pyroclastics, type, quantity, size and morphology of the clasts) is very important for distinguishing the nature of the volcanic activity, modes of fragmentation and transportation of the volcaniclastic material.

Pumice tuff packet. Includes both pyroclastic (ash and lapilli-tuffs with levels of matrix-supported pyroclastic breccias) and epiclastic rocks. The tuffs and pyroclastic breccias contain lithics, free crystals and crystal fragments, and glass shards in greatly varying proportions.

Lithic fragments strongly predominate. The most abundant and overall distributed is highly vesiculated, commonly tube pumice. Pumice clasts vary in size from fine ash to blocks (over 10 cm), but coarse-grained ash and lapilli (0.1–3 cm) normally prevail. The shape of the pumice clasts is irregular, angular, frequently elongated parallel to the fine tube-like vesicles. They often contain microliths, and the larger ones – even phenocrysts, commonly of plagioclase and biotite. Spherical bubble-containing pumice is present in some samples of vitric ash tuffs building separate levels in the northernmost parts of the Sheinovets caldera, to the east of Mezek Village.

Dense rhyolite lava fragments are also very abundant and widely distributed in the whole volume of the pumice tuff packet. They result from disruption of lava that cooled in the conduit or filling the vent. Their size varies in a much wider interval than the pumice clasts but coarse-grained ash and lapilli-sized particles strongly prevail. The rhyolite lithoclasts are angular or slightly rounded, pink or gray in colour. They are holocrystalline – felsitic or rarely spherulitic. Small phenocrysts of plagio-clase and biotite can be seen in the larger lapilli and block-sized clasts. The pyroclastic breccia levels contain abundant rhyolite blocks that rarely exceed 1 m in size. Huge rhyolite blocks more than 10 m in diameter have been found in the southeasternmost parts of Sheinovets caldera, close to the state border. They differ from the rest of observed lithics in quantity and content of the phenocryst assemblage (sample 158, Table 2) including relatively large (up to 5 mm) crystals of plagioclase, biotite, sanidine and amphibole. Rhyolite blocks are massive, showing no flow banding or any spatial orientation of fabric elements.

Andesite fragments are reported by Aleksiev et al. (2000) but such lithics have not been detected during our fieldwork or petrographic studies.

The chemical composition of the present rhyolite lithics has been determined by X-ray fluorescence (XRF) and electron-probe microanalyses (EPMA, area scanning). The results are listed in Table 1 and 3. Due to the restricted area of measuring and the lack of phenocrysts in many of the analyzed lithics, the microprobe results are representative only for the groundmass of fine quartz-feldspar aggregate. This is reflected in low CaO concentrations, lack of MgO and higher K_2O contents and for this reason they plot in the trachyrhyolite field on the TAS-diagram (Fig. 6).

Clasts with perlitic cracks are also of wide occurrence. Since perlites form at or close to the surface, these pyroclastic fragments are always derived from the vent area, i.e. they result from previous non-explosive eruptions. The prevailing sizes are coarse-grained ash and fine-grained lapilli, the latter being not larger than 1 cm. Their rounded shape results from the concentric cracks. “Bodies” composed only by perlite clasts are found at different places within the pumice tuff packet and close to the lava domes. They were identified during the microscopic work and, regarding their macroscopic features, they cannot be distinguished from the surrounding pyroclastics. On the map (Fig. 1) they are indicated as “perlitic breccias” although the dominating particles are lapilli-sized.

Fragments of different metamorphic rocks (xenoclasts) are also present but in small quantity. Their size is about few mm (most often 1-3 mm), although larger clasts 1-2 cm in diameter can be seen within the pyroclastic breccia levels. Normally, they are better rounded, elongated parallel to the cleavage and are represented by gneisses, schists and amphibolites.

Small amounts of crystal clasts are also present. The crystalloclasts are angular fragments and rarely free crystals of plagioclase, biotite, quartz and sanidine. Plagioclase is prevailing. Normally, they are not larger than 2 mm. Single grains of amphibole, zircon, apatite and opaque mineral (most probably magnetite) can be rarely seen. Rounded fragments of metamorphic quartz with wavy extinction and shaded feldspar with abundant inclusions have been also detected.

Table 1. *Major element content of rhyolite lithoclasts from the pyroclastic unit obtained by EPMA (Electron-probe microanalysis) trough area scanning*

Таблица 1. *Химичен състав на риолитови литокласти от пирокластичната задруга, определен с микросонда посредством площно сканиране*

	Pumice tuff packet						Lithic breccia	
No sample	221-1	221-2	160-1	160-2	160-3	6	69-1	69-2
N analyses	3	2	3	1	2	3	1	3
SiO_2	77.33	74.96	76.62	77.51	77.30	76.99	79.85	77.95
Al_2O_3	12.39	14.02	12.79	12.65	12.65	13.08	10.66	12.38
TiO_2	0.16	0.07	0.10	0.34	0.10	0.40	0.23	0.05
Fe_2O_3	0.19	0.40	0.75	0.39	0.42	0.52	0.45	0.48
CaO	0.56	0.60	0.59	0.57	0.32	0.81	0.42	0.26
MgO	-	-	-	-	-	0.09	0.18	-
Na_2O	2.78	2.98	3.01	2.72	2.88	3.69	0.71	3.80
K_2O	5.83	6.96	5.99	5.83	6.53	4.34	7.51	5.08
MnO	0.08	0.05	0.03	-	0.03	-	-	-
BaO	0.05	0.08	0.12	-	-	-		-
total	99.37	100.12	100.00	100.01	100.05	100.00	100.01	100.00

Ash-sized dense particles of volcanic glass are also very abundant. The presence of two types of pumice indicates that two types of vitroclasts were formed. The first of them accompanies the pumice, containing tube-like bubbles. Resulting vitroclasts are extremely fine and have elongated needle-like shapes (Heiken, Wohletz, 1991). After deposition and especially after subsequent welding or alteration, such fragments (as in the case of Sheinovets caldera) form homogeneous mass. Such mass (dark and showing no traces of the initial clast shape) fills in the space between the other pyroclasts and rarely is in significant quantity in the studied samples. Vitroclasts with typical concave outlines, resulting from the presence of spherical bubbles in the erupting magma, form some interbeds to the south and west of Mezek Village and built almost entirely a pyroclastic flow unit detected in the northern parts of the area. They are ash-sized, fine- or coarse-grained.

The huge amount of pumice in the pumice tuff packet suggests significant volumes of associated glassy ash. However, the ash-sized vitroclasts in most of the samples are in quite small quantity. Therefore, it can be assumed that most of the finest ash particles were elutriated from the eruptive column during the eruption or later, during the movement of the pyroclastic material, and were deposited outside the boundaries of the studied area.

The epiclastic rocks in the section of the pumice tuff packet are composed by re-deposited tephra, mainly crystalloclasts and much less vitroclasts, whereas significant amounts of xenoclasts (up to 30%) are locally observed. The matrix is fine-grained and dark under crossed pollars. Sometimes carbonate is present; fossils can also be seen.

Lithic breccia packet. Lithic breccias from the upper packet are diffusely stratified, clast-supported and contain the same types of pyroclasts as the pumice tuff packet but their size and quantitative rations differ significantly.

The most abundant constituents are cognate dense lava fragments of rhyolite composition. Their quantity strongly prevails over that of all other components. The rhyolite clasts vary in size from coarse-grained ash (in the matrix) to blocks about 10-12 cm in diameter. Most abundant are coarse-grained lapilli (>1 cm). They are angular to poorly rounded in the upper levels of the packet.

With respect to their texture, the rhyolite clasts from the lithic breccia packet are similar to those observed in the pumice tuff packet. They are holocrystalline with scarce phenocrysts of plagioclase and biotite. The groundmass is microcristalline, felsitic or spherulitic. The composition of two lithoclasts from the lithic breccia packet (obtained by EPMA, area scanning) is shown in Table 2.

Xenoliths of metamorphic rocks (schists, gneisses, amphibolites), ranging from few mm to 2-3 cm in size, are also abundant. They are much better rounded than the rhyolite clasts and might have been derived from the coarse-grained Priabonian sediments, which are rich in metamorphic fragments and are currently exposed to the west of Sheinovets caldera.

The matrix of the lithic breccias is composed of fine-grained ash-sized pyroclastic material including angular crystal fragments (of feldspars, mainly plagioclase, biotite and quartz), rounded clasts of metamorphic quartz (rarely up to 3-5 mm in size), fine clasts of rhyolite lava and rarely - perlite fragments. The matrix in the lower parts of the packet is enriched in juvenile glassy fragments – pumice (ash- and lapilli-sized both with tube-like and spherical bubbles) and glass shards with typical shape and as large as 1 mm. The quantity of the glassy fragments decreases upward.

A general scheme of the variations in type and observed maximal diameters of the clasts in the section of the pyroclastic unit is shown in Fig. 3.

Petrographic characteristic of volcaniclastic rocks from the Sheinovets caldera rim

Volcaniclastic varieties exposed in the southern flanks of the Ibredjeck horst are studied just to the west of the Sheinovets caldera. The tuffs

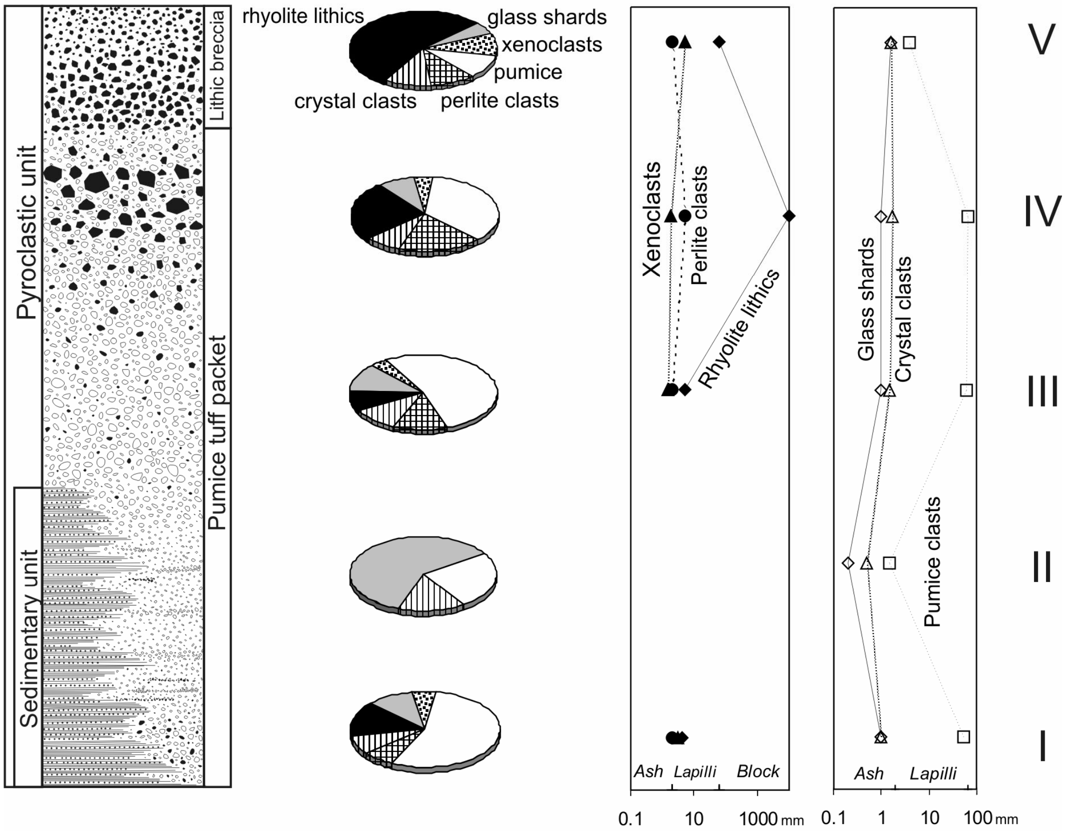

Fig.3. Generalized cross-section of the intracaldera sequence with vertical changes in abundance and maximal diameter of the pyroclasts (in mm). The exposure of the I-V levels is shown in Fig. 2

Фиг. 3. Обобщен профил на изпълващите калдерата материали. Показани са вертикалните изменения в количеството и максималния диаметър на пирокластите (в mm). Положението в план на нивата I-V е показано на картата от фиг. 2

consist almost entirely of ash and rarely contain fine-sized lapilli not larger than few mm. Similarly to the caldera-filling pyroclastics they are built of lithoclasts, crystalloclasts and glass shards, but dense lithics are scarcely present.

Lithoclasts are mainly of ash-sized pumice containing tube-like bubbles. Separate ash- or fine lapilli-sized fragments of angular rhyolite with fine phenocrysts of plagioclase and biotite can also be observed. Ash-sized perlite clasts have been identified in one sample. Tiny fragments of metamorphic rocks (gneisses and amphibolites) are overall distributed.

Table 2. *Abundance, composition and characteristics of phenocrysts in Sheinovets caldera rhyolites*
Таблица 2. *Количество, състав и характер на порфирите в риолитите от Шейновецката калдера*

Location, sample No and phenocryst content	SW of M.-Gradishte village, subvolcanic dyke	S of M. Gradishte village, dome		SE of M.-Gradishte village, dome	Sheinovets peak, dome
	75 (rhyolite) ~30%	365 (rhyolite) ~10%	63 (perlite) ~10%	89 (rhyolite) <5%	1 (rhyolite) ~10-15%
Plagioclase	replaced by calcite, albite, kaolinite and illite			slightly zonal An_{20-15}	
core		strongly cracked and resorbed an_{39-33}	coarse sieve-textured, An_{32-38}		strongly resorbed, An_{42-40}
periphery	-	-	oscillatory zoned An_{48-28}	-	pure potassium feldspar $Ab_{0.4}Or_{99.4}$
outermost rim	-	narrow, slightly zonal An_{37-28}	An_{33-28}	-	narrow, with zonal texture An_{31-28}
Sieve-textured	?	-	-	-	-
Biotite Mg/Mg+Fe	52.4-54.2	60.9-63.1	61.2-62.2	55-55.6	58.4-59.8
Al_{IV}	2.447-2.498	2.46-2.513	2.352-2.518	2.417-2.463	2.44-2.53
Quartz	well rounded	-	-	well rounded	-
Sanidine	slightly rounded Or_{76}	-	-	Or_{67-72}	microlites Or_{58-62}
Amphibole	altered	-	-	-	-
Pyroxene	-	-	-	-	-
Accessories	Zc, Ap, Tit, Mt	Zc	Ap	Zc, Mt	Zc, Ap
Groundmass	altered	felsitic	glassy	granophyric, rich in anhedral Q grains	felsitic with single spherulites

Zc – zircon, Ap – apatite, Tit – titanite, Mt - magnetite

Crystalloclasts are abundant and presented by fine ash-sized fragment of feldspars (mainly plagioclase), quartz and biotite. Tiny glass shards of those associated with the tube-like pumice probably built the abundant matrix, which is compact and dark under crossed pollars. All clasts made of glass are completely replaced, mainly by zeolites.

The fine-grained epiclastic varieties are more abundant in the lower parts of the section. They contain mainly fragments (<<1 mm) of feldspars, biotite and quartz. The matrix is clayey or carbonatic, and the presence of glass shards is uncertain.

Therefore, the grain-size and thickness of the deposits are the only significant differences between the caldera-fill and the pyroclastics exposed in the caldera rim. It can be thus supposed that pyroclastics from the caldera rim are likewise connected to the volcanic activity that initiated the subsidence of Sheinovets caldera.

Table 2. *(Continuation)*
Таблица 2. *(Продължение)*

Location, sample No and phenocryst content	SW of Mezek village, dome		Kushkaya peak, dyke	S of Sheinovets peak, dyke	Lithoclasts from the pyrocl. unit
	169 (rhyolite) <5%	317 (perlite) <10%	198 (rhyolite) <10%	254 (rhyolite) ~15-20%	158 (rhyolite) ~30-35%
Plagioclase			weakly zoned An_{12-24}		
core	An_{41-39}	resorbed "mixture" of An_{78-62} and An_{46}		strongly resorbed "mixture" of An_{84-69} and An_{59-41}	slightly resorbed An_{55-53}
periphery	An_{33-26}	oscillatory zoned An_{40-21}	-	wide, oscillatory zoned An_{76-32}	oscillatory zoned An_{46-25}
outhermost rim	An_{29-26}	An_{27-24}	-	An_{39-38}	An_{30-33}
Sieve-textured	-	$An_{25.9-30.1}$	-	An_{39-31}	An_{33}
Biotite Mg/Mg+Fe Al_{IV}	 58.4-61.1 2.298-2.422	 59.5-60.7 2.373-2.457	 55-55.9 2.424-2.46	 58-61.3 2.407-2.599	 60.2-60.7 2.389-2.434
Quartz	-	-		-	-
Sanidine	-	-	Or_{72-65}	Or_{69}	Or_{71-72}, rarely Or_{99-100}
Amphibole	-	-	-	-	Mg/Fe 0.703-0.801
Pyroxene	-	-	-	$Wo_{48-46}En_{40-37}$	-
Accessories	Mt	Ap, Mt,	Mt	Mt, Ap	Mt, Tit, Zc
Groundmass	microfelsitic	glass with microlites	granophyric, rich in anhedral Q grains	cryptocrystalline	felsitic, rich in microlites (Fs, Bt)

Zc – zircon, Ap – apatite, Tit – titanite, Mt – magnetite

Petrology of the rhyolite lava

The rhyolite lava builds several bodies localized in the northeasternmost and south-westernmost parts of the area. Some E-W trending dykes are arranged along the southern border of the studied area. Several sill-like bodies and dykes are emplaced within the rocks of the breccia-conglomerate unit to the southwest of Malko-Gradishte Village, west of the caldera fault (Fig. 2). On the basis of their K-Ar ages (ranging from 36.71±1.39 to 32.11±1.28 Ma (Ivanova et al., 2001) and listed in Table 3) the Sheinovets caldera rhyolite bodies can be divided into two age groups: 1) Priabonian (Malko-Gradishte), including the bodies from the northern parts of the area and 2) Rupelian (Sheinovets), comprising the domes and dykes emplaced close to the southern border of the area.

Petrographic characteristics

The textures of the caldera rhyolites, especially the presence of perlites in the peripheral parts of some of the bodies, suggests that they cooled at or very close to the surface forming volcanic domes. The presence of perlites within the large dome exposed to the south of Malko-Gradishte Village is indicative of its. poliphase nature and composite structure resulting from the coalescence of several smaller bodies. Two types of transition

Table 3. *Major and some trace element contents in Sheinovets caldera rhyolites. K-Ar ages of some of the bodies are also shown*

Таблица 3. *Химичен състав на риолити от Шейновецката калдера. K-Ar възраст на някои от телата също е показана*

	Malko-Gradishte Group				Sheinovets Group domes							Sheinovets Group dykes					Lithoclasts	
Sample	89	365	365mi	63	1	45	46	144	169	317	317g	182	186	195	198	254	158	215
Lithology	rhyolites			perlite	rhyolites					perlite		rhyolites					rhyolites	
SiO_2	78.85	76.67	79.72	69.87	74.74	77.9	75.16	74.84	78.51	70.82	71.70	75.99	78.51	78.2	79.25	71.08	72.85	77.71
TiO_2	0.07	0.15	0.17	0.16	0.16	0.17	0.20	0.15	0.11	0.13	0.10	0.16	0.13	0.14	0.08	0.29	0.28	0.16
Al_2O_3	10.60	11.46	9.69	13.16	12.91	12.21	13.27	12.65	11.42	12.61	12.34	12.91	11.62	11.92	11.15	14.35	13.92	11.6
Fe_2O_3	0.41	1.13	0.16	1.16	1.10	0.92	1.16	0.70	0.85	0.92	0.55	0.85	0.79	0.59	0.70	2.02	1.89	0.71
MnO	0.03	0.04	0.11	0.10	0.03	0.01	0.11	0.02	0.04	0.08	0.09	0.04	0.04	0.01	0.04	0.08	0.04	n.d.
MgO	0.09	0.27	0.02	0.41	0.28	0.54	0.21	1.15	0.15	0.24	0.06	0.58	0.07	0.80	0.11	0.47	0.49	1.65
CaO	0.37	0.83	0.17	1.51	0.76	0.55	1.08	0.67	0.61	1.09	0.63	0.46	0.44	0.79	0.45	1.93	1.78	0.86
Na_2O	2.56	2.69	0.89	1.47	2.82	1.15	3.24	2.34	3.14	4.00	3.31	2.57	3.47	3.27	2.91	3.71	3.54	2.46
K_2O	5.06	4.83	2.63	4.96	5.77	4.73	4.66	4.83	4.60	3.24	3.34	5.08	4.79	4.32	4.97	4.71	4.54	3.81
P_2O_5	0.02	0.04		0.03	0.05	n.d.	n.d.	n.d.	0.03	0.04		n.d.	0.03	n.d.	0.03	0.10	0.10	n.d.
LOI	0.58	0.55		6.46	0.63	1.39	0.47	2.16	0.27	5.88		0.89	0.38	0.49	0.47	0.30	0.28	0.63
Total	98.64	98.66	93.57	99.29	99.54	99.57	99.56	99.51	99.73	99.05	92.11	99.53	100.27	100.53	100.16	99.04	99.71	99.59
Nb	14	13		14	12				12	12			23		14	16	14	
Zr	45	94		113	98	86	90	114	86	93		136	118	94	54	159	129	111
Y	14	16		18	17	16	19	5	15	18		0	17	14	17	19	14	13
Sr	30	116		386	102	71	129	110	79	118		21	16	100	34	247	224	126
Rb	172	185		125	195	181	151	184	155	251		317	241	157	184	189	165	127
Pb	31	32		27	36				28	40			35		33	39	34	
Ga	9	10		10	11				9	10			10		9	13	13	
Zn	12	28		37	33				28	35			24		20	31	27	
Cu	<3	3		<3	5				<3	<3			<3		<3	5	4	
Ni	<3	<3		<3	<3				<3	<3			<3		<3	<3	<3	
Co	<1	1		2	2				1	2			1		<1	4	3	
Cr	4	<2		<2	<2	0	8	0	<2	<2		19	4	4	4	<2	<2	14
Mn		213		1331	263	247	1372	185	324	1000		402	417	212	250	720	483	86
Sc	2	2		3	2				2	2			0		3	2	2	
V	<2	8		8	9	8	8	10	2	4		21	<2	10	<2	23	23	29
Ti		685		858	1084	881	833	797	555	740		897	663	595	566	1510	1656	701
Ce	32	52		56	57				58	65			73		37	63	58	
Ba	330	938		1087	1091	853	711	535	1140	1172		0	45	1067	382	1312	1447	742
La	8	25		28	25				28	34			36		15	35	31	
K-Ar age (Ma)	36.73 ±1.39	35.24 ±1.33			32.94 ±1.29				33.18 ±1.31				32.38 ±1.37			32.45 ±1.37		

mi- composition of melt inclusion in plagioclase phenocryst; g – composition of perlite glass

mi- състав на стъклено включение в плагиоклазов порфир; g – състав на стъклото between the rhyolite core and perlite peripheries have been detected. Alternation of felsitic rhyolite and perlite layers of different thickness is typical of the domes, whereas rhyolite spherulites enclosed in perlite matrix occur in the peripheries of the dykes.

The caldera rhyolites are light gray or pink, massive, showing no spatial orientation of fabric elements, or flow-layered by alternating, differently coloured (light and dark pink) thin layers, ranging in thickness from <1 mm to 4-5 mm. Locally the flow layering is accompanied by thin (<1-1.5 cm) planar jointing. Where it is present, the flow banding is always steep or vertical and parallel to the margins of the domes.

The rhyolites are porphyritic with low phenocryst contents. The phenocryst assemblage consists of plagioclase and biotite (± sanidine, quartz, amphibole and pyroxene). Plagioclase is most abundant and occurs as variously zoned crystals sometimes displaying significant compositional variation (Fig. 4a). Compositionally homogeneous sieve-textured crystals are also present (Fig. 4b). The accessory minerals detected are magnetite, apatite and zircon. A brief description of phenocrysts is given in Table 2.

The groundmass is felsitic, represented by fine-grained quartz-feldspar aggregate. Microlites of sanidine are sometimes present. The spherulitic texture is more typical of the dykes but separate small spherulites can be rarely seen in dome rhyolites. The groundmass in the perlite varieties consists of fresh glass rich in plagioclase microlites. The composition of perlite glass from one dome of Sheinovets group is shown in Table 3.

The caldera rhyolites are either fresh, showing no traces of hydrothermal alteration, or slightly affected by secondary processes resulting in precipitation of opal-CT, adularia and albite in tiny fractures within the plagioclase phenocrysts. The concentric cracks, typical of perlite varieties, are filled by clay minerals.

The rhyolites, exposed within the breccia-conglomerate unit in the rim of the Sheinovets caldera, form numerous sill-like bodies and dykes less than 10-15 m thick. Locally they show prismatic jointing. They are light, beige or white in colour, coarse porphyritic and strongly altered (Fig. 4c). The phenocryst assemblage is represented by sanidine, biotite and quartz. Plagioclase and amphibole are completely altered but their euhedral outlines still can be easily detected. On the base of the abundance (nearly 25-30%) and larger size of the phenocrysts, their strong hydrothermal alteration and position in the basement of the studied volcanics, the sill-like bodies and dykes from the caldera rim are assumed to be subvolcanic.

Temperature of crystallization, pressure and pre-eruptive water contents

Coexisting sanidine and plagioclase in some of the samples allow applying the two-feldspar geothermometer of Fuhrman and Lindsley (1988). Calculated temperatures from the plagioclase-sanidine pairs in two samples are 660 and 675°C.

The pressure, at which the amphibole in the lithoclasts from the pumice tuff packet was formed, has been estimated on the basis of its Al content using the equation of Johnson and Rutherford (1989). The obtained results vary significantly from 0.8 to 2.9 kbar. Plotted on the Al/Si_{Amph} *vs.* Al/Si_{Pl} diagram (Fershtater, 1990), which displays the distribution of Al and Si between coexisting plagioclase and amphibole, the composition of these minerals indicates pressure of about 2 kbar (Fig. 5), corresponding to depths of about 6-7 km. It should be mentioned that not the cores but the peripheral parts of plagioclase crystals are supposed to be in equilibrium with amphibole based on the composition of plagioclase grains (An_{29}) trapped by growing amphibole (Fig. 4d).

Highly dominating explosive activity in the area, which produced abundance of vesiculated pumice, argues for a water-rich magma. Quantity of few percents water can be supposed on the basis of the composition of a melt inclusion trapped in a plagioclase phenocryst from the Malko-Gradishte dome

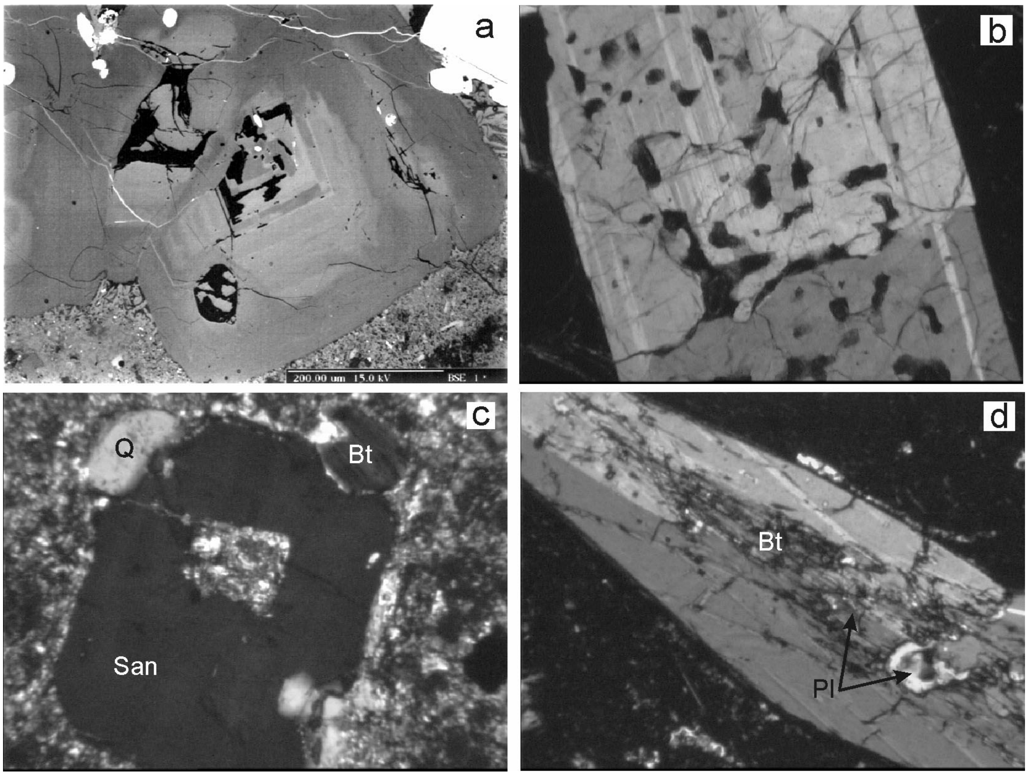

Fig. 4a. Back-scattered electron image of oscillatory zoned plagioclase (sample 254). Black areas in the centre are of opal-CT. Microphotographs (× N, 1.3 mm wide): b. Coarse sieve-textured plagioclase (sample 317); c. Altered euhedral plagioclase trapped by lightly rounded sanidine (sample 75); d. Amphibole phenocryst grown on biotite and plagioclase (sample 158). Q – quartz, Bt – biotite, San – sanidine, Pl - plagioclase

Фиг. 4а. Изображение в режим на обратноотразени електрони на плагиоклаз с осцилаторна зоналност (обр. 254). Тъмните участъци в центъра са от опал-СТ. Микроскопски снимки (× N, 1,3 mm широки): b. Ситовиден плагиоклаз (обр. 317); c. Променен автоморфен плагиоклаз, включен в заоблен санидин (обр. 75); d. Амфиболов порфир, нараснал върху биотит и плагиоклаз (обр. 158)

(Table 3), although some loss of alkalis during measurement should be also taken into consideration. The lack of quartz in the phenocryst assemblage of the studied rocks could be also indicative of relatively high pre-eruptive water content of Sheinovets caldera magma, as it was supposed for Arda group acid volcanics (Yanev et al., 1983; Yanev, 1998).

Rhyolite chemistry

The major and some trace element contents of the studied rocks are listed in Table 3. Based on the (K_2O+Na_2O) *vs* SiO_2 diagram (Le Maitre et al., 1989) all samples are rhyolites or either rhyolites or trachyrhyolites according to the modified TAS diagram of Yanev, Andreev (1998) where the field of rhyodacites is also shown (Fig. 6a). As mentioned above, the lithic clasts from the pyroclastic unit plot mainly in the field of trachyrhyolites due to the method of measurement and the small size of the measured area. The Sheinovets caldera rhyolites are high-K as shown on the K_2O *vs.* SiO_2 diagram (Fig. 6b, Le Maitre et al., 1989).

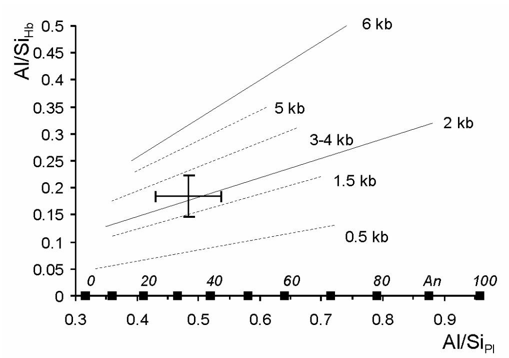

Fig. 5. Evaluation of pressure using Al/Si ratio in coexisting amphibole and plagioclase (Fershtater, 1990)
Фиг. 5. Диаграма за оценка на налягането според отношението Al/Si в съсъществуващи амфибол и плагиоклаз (Ферштатер, 1990)

It should be also noted that some increase of alkali contents could be due to presence of adularia and/or albite although their amount is too low to cause significant changes in the contents of K_2O and Na_2O. Most of the major oxides, except for K_2O showing no variation, decrease more or less significantly with increasing silica resulting probably from the fractionation of the detected mineral phases (Fig. 7). Scatter in the plots of MgO and CaO may reflect analytical errors due to the relatively low contents of these elements in the rocks. Samples rich in TiO_2 and P_2O_5 are those having higher phenocryst contents and, respectively, containing higher amount of accessory minerals. Plotted against SiO_2, trace elements also show negative correlation (best expressed for Sr) related to possible fractionation of plagioclase and accessory phases (Fig. 8). Similar to K_2O, Rb does not vary significantly with increasing SiO_2. The low Y contents, typical of all Maritza group volcanics, are explained by fractionation of amphibole (Yanev, 1998). Some contribution of apatite can be also of significance presuming the higher apatite-melt K_D^Y value (40; Rollinson, 1993) for acid melts. Fractionation of a mineral assemblage dominated by plagioclase and including also amphibole, biotite and accessories but no K-feldspar may be involved in the magma evolution on the basis of the Harker's diagram and the plots shown in Fig. 9.

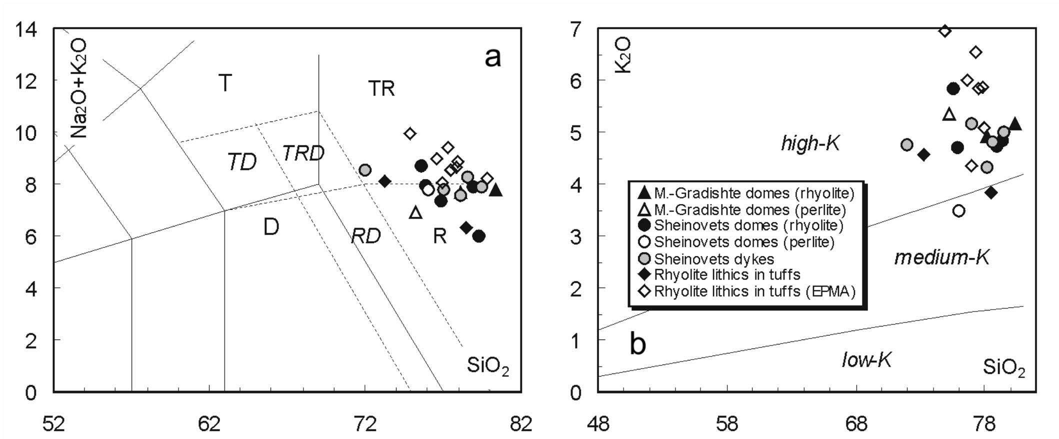

Fig. 6. Classification of the Sheinovets caldera volcanics. a. TAS diagram (Le Maitre et al., 1989, modified by Yanev and Andreev, 2000); b. K_2O *vs*. SiO_2 diagram (Le Maitre et al., 1989)
Фиг. 6. Класификация на вулканските скали от Шейновецката калдера. a. TAS диаграма (по Le Maitre et al., 1989, допълнена от Yanev & Andreev, 2000); b. Диаграма K_2O-SiO_2 (Le Maitre et al., 1989)

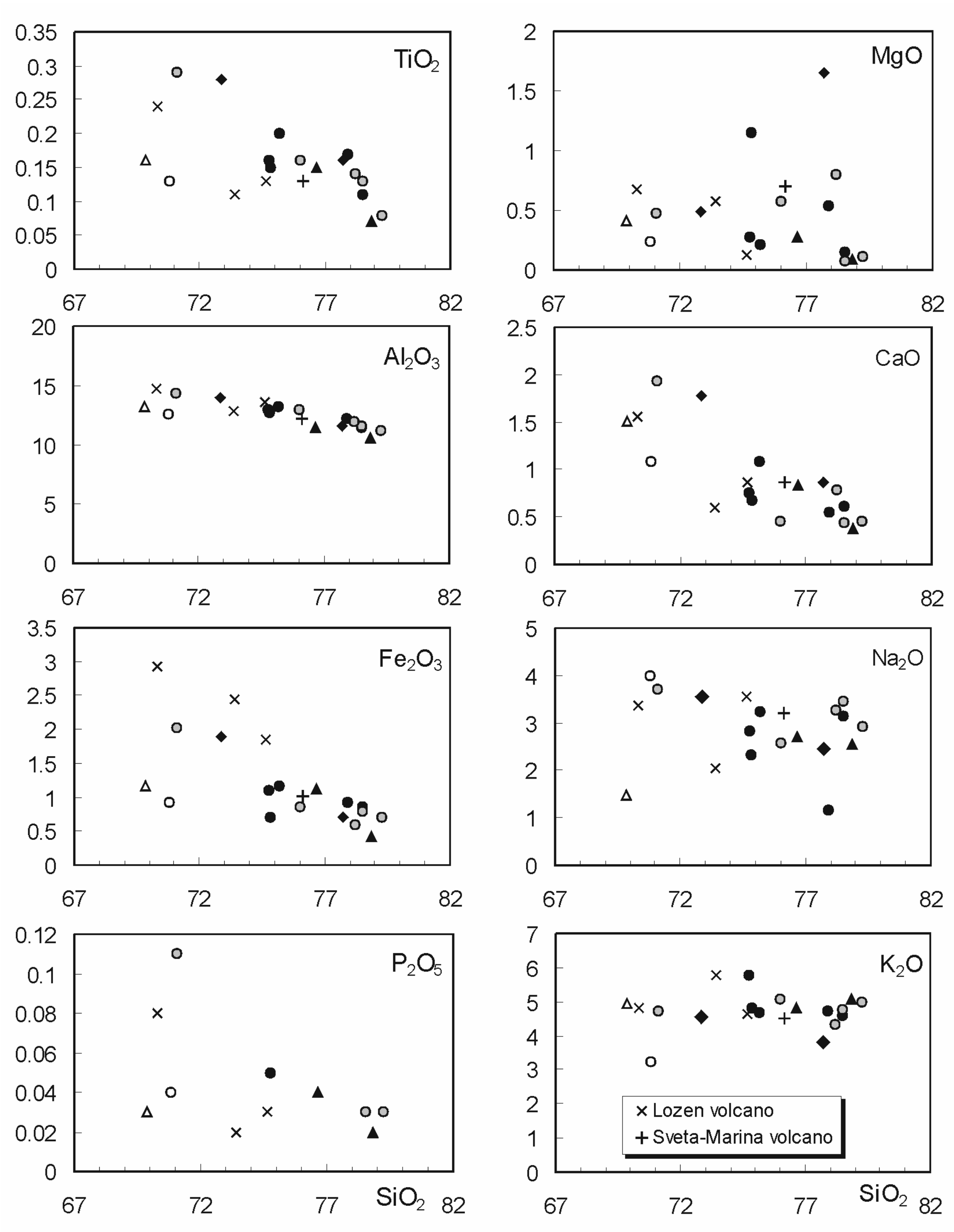

Fig. 7. Harker's diagrams (major oxides) for the Sheinovets caldera rhyolites. The Lozen and Sveta-Marina volcanics (data of Yanev, 1998) are also plotted for comparison. Symbols are the same as in Fig. 6

Фиг. 7. Харкерови диаграми (основни оксиди) за риолитите от Шейновецката калдера. За сравнение са показани и проекциите на вулканитите от Лозен и Света Марина (по данни наYanev, 1998). Символите са като на фиг. 6

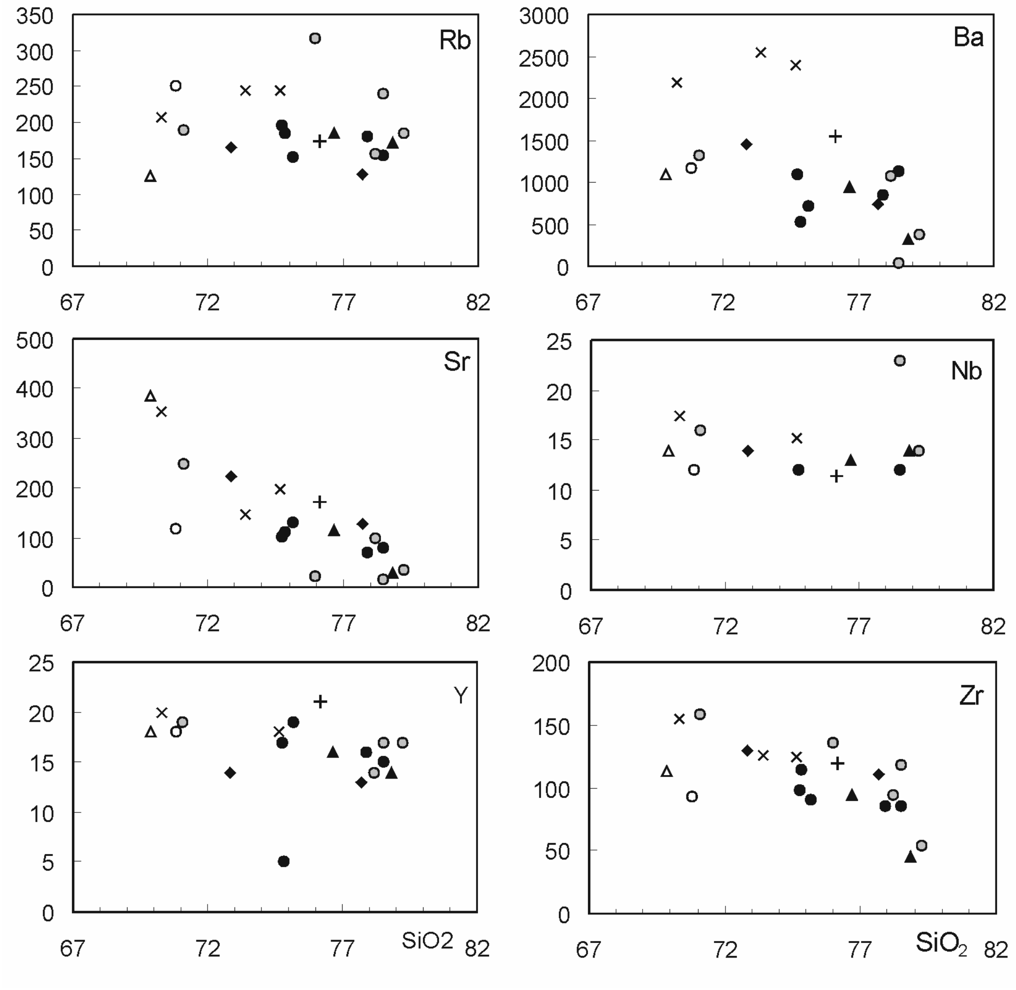

Fig. 8. Selected Harker's diagrams (trace elements) for the Sheinovets caldera rhyolites. Symbols are the same as in Figs. 6 and 7

Фиг. 8. Избрани харкерови диаграми (елементи-следи) за риолитите от Шейновецката калдера. Символите са като на фиг. 6 и 7

Geodynamic implications

The geodynamic discrimination of acid highly evolved magmatic rocks is complicated especially when collision-related assemblages are considered (Pearce et al., 1984; Dudas, 1992). This is well demonstrated in the enclosed diagrams (Fig. 10) where acid volcanic rocks from Maritsa group plot in the fields of collision-related and volcanic-arc granites. The Rb-Hf-Ta diagram (Harris et al., 1986) discriminates the rhyolites from Lozen and Sveta-Marina volcanoes as collision-related. This could be also assumed for the Sheinovets caldera volcanics on the base of their geochemical similarity and both spatial and temporal proximity. Presuming that trace element discrimination diagrams reflect distinct

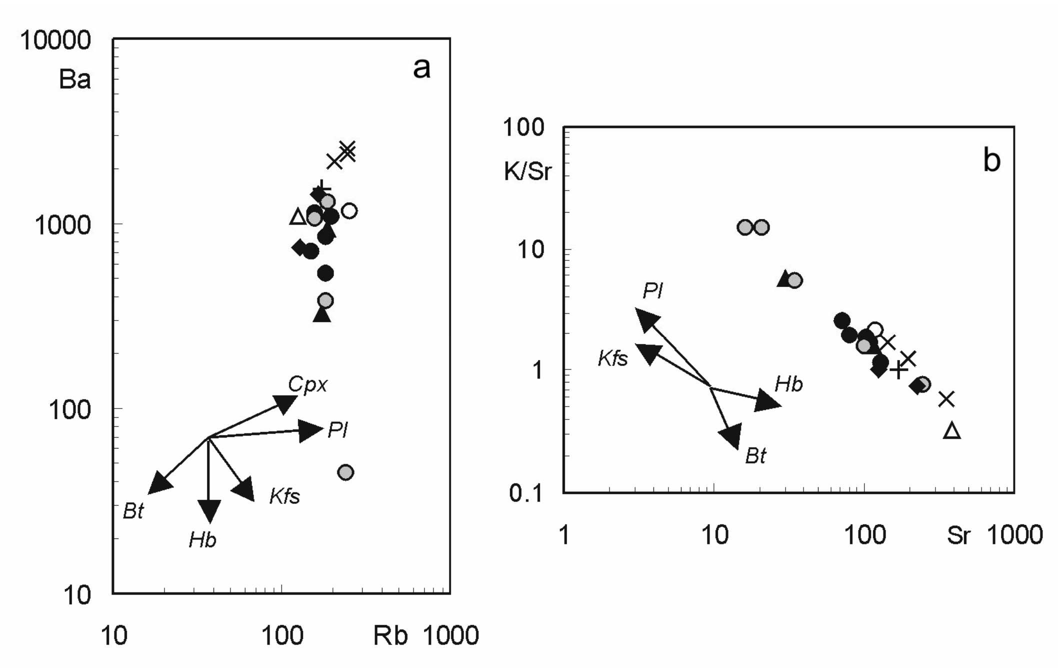

Fig. 9. Ba *vs*. Rb (a) and K *vs*. Sr (b) diagrams with fractionation vectors for biotite (Bt), amphibole (Hb), K-feldspar (Kfs), palgioclase (Pl) and clinopyroxene (Cpx). Symbols are the same as in Figs. 6 and 7
Фиг. 9. Диаграми Ba-Rb (a) и K-Sr (b) с векторите на фракциониране на биотит (Bt), амфибол (Hb), калиев фелдшпат (Kfs), плагиоклаз (Pl) и клинопироксен (Cpx). Символите са като на фиг. 6 и 7

chemical source regions rather than separate geodynamic environments (Pearce et al., 1984), the features of collision-related magmas are explained with involvement of both arc and collisional sources in their formation (Sylvester, 1989). This is in good agreement with the existing hypothesis on the origin of Paleogene magmatics in the Eastern Rhodopes (Yanev et al., 1995).

Discussion and conclusions

Explosive activity

Magma fragmentation. The overall distribution and significant abundance of pumice clasts in the lower pumice tuff packet indicate explosive (magmatic) fragmentation processes resulting from the sudden decompression of rising pumiceous magma (Heiken, Wohletz, 1991). Magma/water interaction could also have played a role in magma disruption, presuming the marine basin proximity although no unambiguous evidence of phreatomagmatic explosions (as accretionary lapilli or base surge deposits) has been found.

The increase of rhyolite lava clast abundance in the upper parts of the pyroclastic section indicates changes in magma fragmentation mechanisms. Overpressure driven explosive destruction of vent blocking solidified rhyolite bodies could have generated the lithic-saturated upper packet. Gravitational collapses or interaction with water could have been also involved in the lava fragmentation process (Cas, Wright, 1988).

Transport mechanisms. The significant thickness, massive structure and poor sorting of the studied rocks are typical of pyroclastic flow deposits. Two different modes of origin, corresponding to the two packets of the pyroclastic unit, have been earlier proposed by Ivanova et al. (2000).

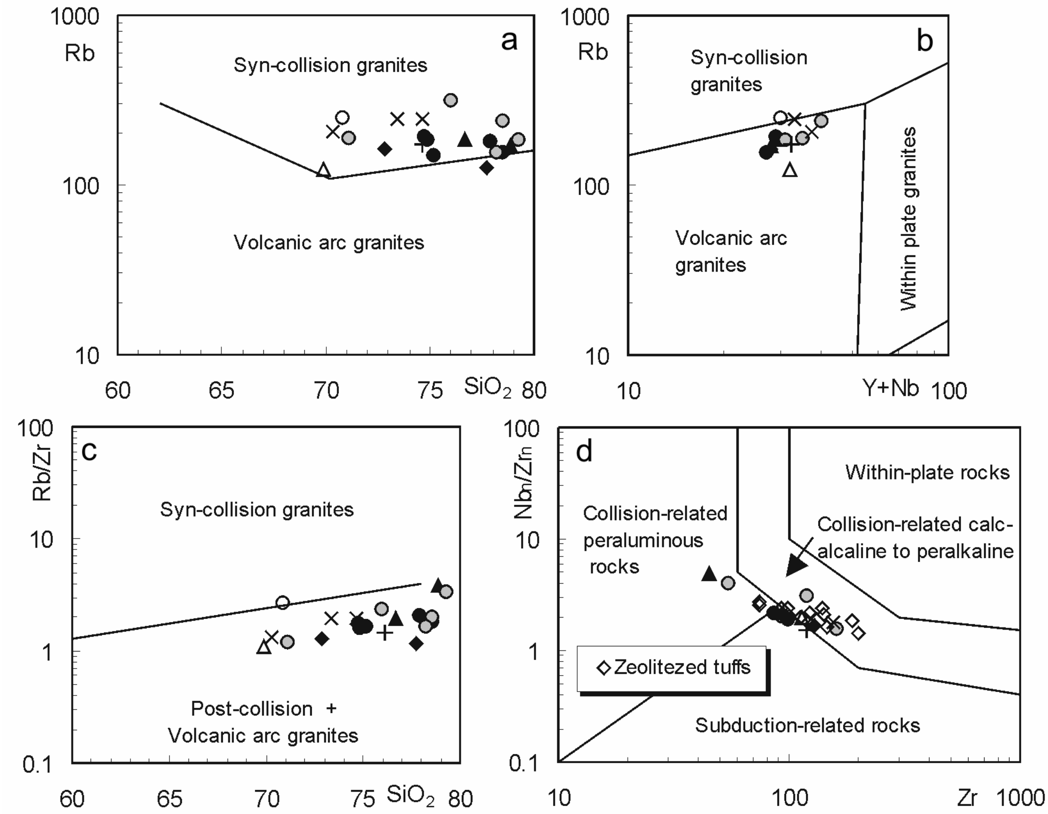

Fig. 10. Maritsa group volcanics plotted in selected discrimination diagrams: a. Rb *vs*. SiO_2 and b. Rb *vs*. Y + Nb diagrams after Pearce et al., (1984). c. Rb/Zr *vs*. SiO_2 plot of Harris et al. (1986). d. Nb_n/Zr_n *vs*. Zr diagram of Thieblemont and Tegyey (1994). Nb and Zr contents are normalized to Nb and Zr values to the primordial mantle (after Hofmann, 1988). Symbols are the same as in Figs. 6 and 7

Фиг. 10. Проекция на вулканитите от Маришката група на избрани дискриминационни диаграми: a. Rb - SiO_2 и b. Rb – Y + Nb по Pearce et al., (1984). c. Rb/Zr - SiO_2 по Harris et al., (1986). d. Nb_n/Zr_n vs. Zr по Thieblemont & Tegyey (1994). Съдържанията на Nb и Zr от последната диаграма са нормализирани към стойностите на Nb и Zr в примитивна мантия (по Hofmann, 1988). Символите са същите, както на фиг. 6 и 7

The rocks from the pumice tuff packet are considered as ignimbrites, deposited in shallow marine environment from dense pyroclastic flows, generated by Plinian column collapse. The lack of bomb sags beneath the large lithoclasts is also an indicator of flow movement. Perlitic breccias can be either pyroclastic flow deposits or elements of outermost brecciated parts of not exposed or already eroded rhyolite bodies.

The lithic breccias from the upper packet seem to be deposited by the so-called blocks- and ash-flows (or rocks avalanges), formed during emplacement and growth of rhyolite domes through directed blasts, explosive or gravitational dome collapses.

Pyroclastic breccias composed mainly of lava clasts with matrix- or grain-supported texture form together with, and represent a part of ignimbrites (Wright, Walker, 1977; Druitt, Sparks, 1982). They can form lens-like bodies sometimes of significant size and tens of meters thick. Vertically and laterally they grade into associated ignimbrites but can also form separate deposits close to the vents (Druitt, Sparks, 1982). According to these authors, they originate from either segregation of the dense clasts within the volume of the less dense fluidized pyroclastic flows or their settlement from the fluidized and diluted flow front. This origin is very likely for the pyroclastic breccias from the pumice tuff packet and could be also an alternative for the rocks of the lithic breccia packet although associated ignimbrites are lacking and significant lateral variations in their petrographic features are not observed.

Some diffusely layered beds, built up by ash-grained pumice and located in the lower part of the pumice tuff packed, are thought to be fall-out deposits (Ivanova et al., 2000). The fine-grained pyroclastic rocks exposed in the caldera rim can be also interpreted as fall deposits that might have fixed the finest ash from downwind plume. The presence of pyroclastic material in the drill cores from the adjacent areas (Kojumdjieva, Dikova, 1980) confirm the idea of a wider distribution of the finest pyroclastic material that must have been erupted during the Sheinovets caldera collapse.

Caldera collapse. Subsidence of the roofs over shallow-seated magma reservoirs after their partial evacuation caused by voluminous ignimbrite eruptions is a common stage in the evolution of silicic magma systems (Walker, 1984; Lipman, 1997). The observed features of the pumice tuff packet: great thickness, massive texture, coarse-grained nature with presence of co-ignimbrite breccias and vertical changes in textural and lithofacial characteristics suggesting an increase in eruption intensity and mass flux; are typical of the so-called caldera-collapse ignimbrites (Cas, Wright, 1988; Rosi et al., 1996; Allen, 2000, etc.). This, together with the registered subsidence with respect to the Priabonian sedimentary units exposed to the west within the Ibredjeck horst, is thought to indicate Sheinovets caldera collapse.

The precise time position of the caldera subsidence is difficult to infer but it can be correlated with the upper parts of the pumice tuff packet where the largest sizes of dense lithics have been detected.

Vent(s) location. No ignimbrite source area has been localized in the currently exposed part of the Sheinovets caldera but on the basis of the eastward increase of the maximum size of lithic clasts it was supposed that the vent region is located to the east of the studied field (Ivanova et al., 2000). The observed vertical changes in lithofacial characteristics of the accompanying sedimentary rocks (changing from fine-grained terrigeneous sediments at the base of the section, recording quiet sedimentation, to reef and detrital limestones needing shallower and in the latter case highly energetic coastal depositional setting) indicate a general tendency of shallowing of the marine basin with the increase of eruptive intensity. This suggests that, in the early stages of eruptive activity, water might have had access to the vent. The degree of water/magma interaction during a submarine eruption depends on the mass flux rate (Allen, 2000; Wohletz et al., 1995) and possible occurrence of solidified lava bodies in the conduit and vent. Unrestricted access of water to the vent in our case is supposed to have taken place during the initial eruptive stages (not recorded in the currently exposed section; Ivanova et al., 2000). Later, the increase of the eruptive (both explosive and effusive) intensity, resulting in lower efficiency of magma/water interaction, contributed only to the high degree of magma fragmentation registered in lower parts of the pyroclastic unit.

Effusive activity and an approach to magma chamber processes

The abundance of cognate rhyolite lava and perlite fragments in the whole pyroclastic section indicates that explosive events alternated with periods of relatively quiet eruptions of rhyolite lava at or very close to the surface. Several models are proposed to explain complex eruptive behavior of acid volcanic systems resulting from changes of volatile content and magma accent rate on an eruptive timescale (Fink, 1983; Eichelberger et al., 1986; Woods, Koyaguchi, 1994, etc.). The internal stratigraphy and texture of the pyroclastic unit show that dome growth was the dominating eruptive style in later post-collapse stages of Sheinovets caldera evolution (Ivanova et al., 2000). Such a transition from mainly explosive activity to a regime of lava extrusion is normally observed at many silicic volcanic centers (Jaupart, Allègre, 1990; Eichelberger, 1995, etc.).

The high uniformity of lithic pyroclasts and their similarity (both textural and compositional) to currently exposed rhyolite bodies argue for a significantly homogenized magma chamber, although gradients must have existed in volatile content, crystal assemblage and degree of contamination by more mafic magma. Except for the wall zones (from where the phenocryst-enriched samples might have been derived) the magma was relatively crystal-poor. Plagioclase and biotite were the main crystals present, accompanied by smaller amounts of sanidine, quartz, amphibole, pyroxene, Fe-oxide and accessories. Amphibole was stabilized by higher water contents in the upper parts of the chamber located at depths of about 6-7 km according to pressure calculation using Al content in coexisting plagioclase and amphibole phenocrysts (Fig. 5). This can explain the abundance of amphibole phenocrysts in earlier eruptive products (Lozen volcano). Amphibole is scarcely seen in later Sheinovets caldera volcanics where it is totally absent from rhyolite lavas (Table 2). This could also be due to very slow accent or long magma storage at shallower levels (Rutherford, Hill, 1993). Pyroxene, identified only in the latest eruptive products (Sheinovets dykes), seems to be present in the deeper parts of the chamber where magma was drier and strongly affected by the input of mafic melt from depth. The increase of anorthite content in cores of plagioclases from Sheinovets caldera rhyolites with the progress of volcanic activity (i.e. with withdrawal from deeper magma levels) from An_{55} in rhyolite lithoclasts in ignimbrites to An_{84} in dykes also suggests a process of magma mixing in the lower parts of the chamber. The established sharp leap in the stability field of orthoclase, recorded as a zone of almost pure potassium feldspar within growing plagioclase phenocrysts in one of the Sheinovets domes (Table 2), could be due to contamination by rich in K wall-rock material. This indicates that processes as melting and assimilation might have also occurred during magma storage.

Variations in magma ascent rate and storage of magma batches at shallower levels after some decompression, combined with the nucleation behaviour of silicic melts, can further explain the observed diversity in phenocrysts assemblages and textural characteristics of Sheinovets caldera rhyolite lavas (Swanson et al., 1989; Blundy, Cashman, 2001, Brugger et al., 2003; Martel, Schmidt, 2003, etc.). These questions will be discussed in detail in another publication.

All these data are in agreement with the proposed by Yanev (1998) existence of a large and long-lived magma chamber that has fed all Maritsa group volcanoes. The magma reservoir is thought to have resulted from crustal melting caused by intrusion of intermediate magmas in the crust as the observed geochemical features are explained with extensive plagioclase + minor amphibole fractionation. The earliest eruptive products, Priabonian in age, build the Lozen volcano (Harkovska et al., 1975; 35.6-35 Ma according to Lilov et al., 1987) and possibly also both domes and dykes from the northern parts of the Sheinovets caldera (Malko-Gradishte group), as proposed by Ivanova et al. (2001). At that time the chamber was probably smaller and less acidic melts (up to rhyodacites, II phase of Lozen volcano) coming from deeper parts could easily reach the surface. Gradually, the magma chamber became larger and better homogenized and in the end of the Priabonian and the beginning of the Rupelian (34-33 Ma, Ivanova et al., 2000; 2001) the peak of the volcanic activity shifted slightly to the south where the ejection of huge amount of pyroclastic material led to the

Sheinovets caldera collapse. Rhyolite domes were emplaced both within and outside (Sveta-Marina dome) the caldera (33-32 Ma). The position of the Sheinovets dykes (32 Ma) within the caldera but along the southern fault border of the Ibredjeck horst suggests that the last eruption might have been tectonically induced.

Acknowledgments: The author is deeply indebted to Prof. Dr. W. Richter, Prof. Dr. T. Ntaflos and P. Nagl of Institute of Petrology, Vienna University, for the invitation and assistance with microprobe and XRF analyses. Thanks are also due to W. Füzi and C. Nachtnebel for sample preparation. Helpful comments of Ass. Prof. Y. Yanev and the critical review of Ass. Prof. Dr. P. Marchev are also highly appreciated. Prof. Dr. H. Dabovski is thanked for improving the English version of the manuscript.

References

Aleksiev, B., E. Djourova. 1995. Mordenite zeolites to the west of the town of Svilengrad in the NE Rhodopes, Bulgaria. In: *Sofia Zeolite Meeting'95 Intern. Symp.,* Abstr., p. 3.

Aleksiev, B., E. Djourova, Z. Milakovska-Vergilova. 2000. Zeolitic rocks from the Mezek Mountain, NE Rhodopes. *Ann. Univ. Sofia, Fac. Geol.-Geogr., 1 – Geol.*, **92**, 157-165.

Allen, S.R. 2000. Reconstruction of a major caldera-forming eruption from pyroclastic deposit characteristics: Kos Plateau Tuff, eastern Aegean Sea. *J. Volcanol. Geotherm. Res.*, **105**, 141-162.

Barbiery, M., F. Castorina, U. Masi, C. Garbarino, M. Nicoletti, A. Kassoli-Fournaraki, A. Filippidis, S. Mignardi. 2001. Geochemical and isotopic evidence for the origin of rhyolites from Petrota (Northern Thrace, Greece) and geodynamic significance. *Chem. Erde*, **61**, 13-29.

Berggren, W.A., D.V. Kent, C.C. Swisher, III, M.P. Aubry. 1995. A revised Cenozoic geochronology and chronostratigraphy. In: *Geochronology, Time Scales and Global Stratigraphic Correlation*. Soc. Sedim. Geol., Spec. Publ., **54**, 129-212.

Blundy, J., K. Cashman. 2001. Ascent-driven crystallization of dacite magmas at Mount St Helens, 1980-1986. *Contrib. Mineral. Petrol.*, **140**, 631-650.

Bogdanov, K. 1983. Endogene zonality in the Lozen Ore Field, Eastern Rhodope Mountains. *Ore-Form. Process. Miner. Deposits*, **18**, 48-60 (in Bulgarian with an English abstract).

Boyanov, I., B. Mavroudchiev, I. Vaptsarov. 1963. On the structural and formational peculiarities of part of the Eastern Rhodopes. *Bull. Geol. Inst.*, **12**, 125-186 (in Bulgarian with an English abstract).

Boyanov, I., D. Kozhoukharov, A. Goranov, E. Kozhoukharova, M. Ruseva, J. Shilyafova. 1992. *Explanatory Note to the Geological Map of Bulgaria on scale 1:100 000; Haskovo Map Sheet*. Com. Geol. And Min. Res., Geology & Geophysics Corp., 70 p. (in Bulgarian with an English abstract).

Brugger, C.R., A.D. Johnston, K.V. Cashman. 2003. Phase relations in silicic systems at one-atmosphere pressure. *Contrib. Mineral. Petrol.*, **146**, 336-369.

Cas, R.A.F., J.V. Wright. 1988. *Volcanic Successions; Modern and Ancient*. London, Chapman and Hall, 528 p.

Dudas, F. 1992. Petrogenetic evaluation of trace element discrimination diagrams. In: M.J. Bartholomew et al. (Eds.). *Basement Tectonics: Characterization and Comparison of Ancient and Mesozoic Continental Margins*, Proc. 8th Intern. Conf. on Basement Tectonics, Butte, Montana, 1988. Dordrecht, Kluwer, 93-127.

Druitt, T.H., R.S.J. Sparks. 1982. A proximal ignimbrite breccia facies on Santorini, Greece. *J. Volcanol. Geotherm. Res.*, **13**, 147-171.

Eichelberger, J.C., 1995. Silicic volcanism: Ascent of viscous magmas from crustal reservoirs. *Annu. Rev. Earth Planet. Sci.*, **23**, 41-63.

Eichelberger, J.C., C.R. Carrigan, H.R. Westrich, R.H. Price. 1986. Non-explosive silicic volcanism. *Nature*, **323**, 16, 598-602.

Fershtater, G.B., 1990. Empirical hornblende-plagioclase geobarometer. *Geochemistry*, **3**, 328-335 (in Russian).

Filippidis, A., A. Kassoli-Fournaraki, A. Tsirambides. 1995. The zeolites of Petrota and Metaxades (Thrace) and the kaolins of Leucogia (Macedonia), Greece. In: B. Aleksiev (Ed.). *Sofia Zeolite Meeting'95. Intern. Symp.,* Guide Field Trip, 49-62.

Fink, J. H. 1983. Structure and emplacement of a rhyolitic obsidian flow: Little Glass Mountain, Medicine Lake Highland, Northern California. *Geol. Soc. Am. Bull.*, **94**, 362-380.

Fuhrman, I., P. Lindsley. 1988. Ternary feldspar modeling and thermometry. *Amer. Mineral.*, **73**, 201-215.

Harkovska, A., Y. Yanev, P. Dikova. 1976. Acid volcanism of Late Eocene (Priabonian) age in Eastern Rhodopes Paleogene depression. *C. R. Acad. bulg. Sci*., **29**, 4, 579-582 (in Russian).

Harris, N.B.W., J.A. Pearce, A.G. Tindle. 1986. Geochemical characteristics of collision-zone magmatism. In: M.P. Coward, A.C. Ries (Eds.). *Collision Tectonics*, Geol. Soc. Spec. Publ., **19**, 67-81.

Heiken, G., K. Wohletz. 1991. Fragmentation processes in explosive volcanic eruptions. In: *Sedimentation in Volcanic Settings*, SEPM Spec. Publ., **45**, 19-26.

Hofmann, A.W. 1988. Chemical differentiation of the Earth. The relationship between mantle, continental crust and oceanic crust. *Earth Planet. Sci. Lett*., **90**, 297-314.

Ivanov, R. 1960. Magmatism in the Eastern Rhodopes Paleogene depression. Part I – Geology. *Trav. Geol. Bulgarie, Ser. Geochim., Pol. Izkop*., **1**, 311-387 (in Bulgarian with German abstract).

Ivanova, R., K. Stoykova, Y. Yanev. 2000. Acid pyroclastic rocks from the Sheinovets caldera, Eastern Rhodopes: Lithostratigraphy, characteristics and age. *Geochem. Mineral. Petrol*., **37**, 47-56.

Ivanova, R., Z. Pecskay, Y. Yanev. 2001. K-Ar age of the volcanic rocks from the Sheinovets caldera, Eastern Rhodopes (South Bulgaria). *C. R. Acad. bulg. Sci*., **54**, 3, 59-62.

Ivanova, R., Y. Yanev, Tz. Iliev, E. Koleva, T. Popova, N. Popov. 2001. Mineralogy, chemistry and ion-exchange properties of the zeolitized tuffs from the Sheinovets caldera, Eastern Rhodopes (South Bulgaria). Stud. Surf. Sci. Catal. Amsterdam, Elsevier, 135.

Jaupart, C., C.J. Allegre. 1991. Gas content, eruption rate and instabilities of eruption regime in silicic volcanoes. *Earth Planet. Sci. Lett*., **102**, 413-429.

Johnson, M.C., M.J. Rutherford. 1989. Experimental calibration of the aluminium-in-hornblende geobarometer with applications to Long Valley caldera (California) volcanic rocks. *Geology*, **17**, 837-841.

Kirov, G.N., A. Filippidis, A. Tsirambidis, R.G. Tzvetanov, A. Kassoli-Fournaraki. 1990. Zeolite-bearing rocks in Petrota area (Eastern Rhodope massif, Greece). *Geol. Rhodopica*, **2**, 500-511.

Kojumdjieva, E., P. Dikova. 1980. Paleogene sediments of borehole R-1 Svilengrad. *Geol. Balcanica,* **10**, 2, 107-110.

Kozhoukharov, D., I. Boyanov, E. Kozhoukha-rova, A. Goranov, S. Savov, G. Shilyafov. 1995. *Explanatory Note to the Geological Map of Bulgaria on scale 1:100 000; Svilengrad Map Sheet*. Com. Geol. And Min. Res., Geology & Geophysics Corp., 67 p. (in Bulgarian with an English abstract).

Le Maitre, R.W. (Ed.) 1989. *A Classification of Igneous Rocks and Glossary of Terms*. Recommendations of the IUGS Subcommission on the systematics of igneous rocks. Oxford, Blackwell, 193 p.

Lilov, P., Y. Yanev, P. Marchev. 1987. K/Ar dating of the Eastern Rhodope Paleogene magmatism. *Geol. Balcanica*, **17**, 6, 49-58.

Lipman, P.W. 1997. Subsidence of ash-flow calderas: Relation to caldera size and magma chamber geometry. *Bull. Volcanol*., **59**, 198-218.

Martel, C., B.C. Schmidt. 2003. Decompression experiments as an insight into ascent rates of silicic magmas. *Contrib. Mineral. Petrol*., **144**, 397-415.

Martini, E. 1971. Standard Tertiary and Quater-nary calcareous nannoplankton zonation. In: *Second Planktonic Conf*., Rome, Proc., 739-785.

Pearce, J.A., N.B. Harris, A.G. Tindel. 1984. Trace element discrimination diagrams for the tectonic interpretation of granitic rocks. *J. Petrol*., **25**, 956-983.

Rollinson, H. 1993. *Using Geochemical Data: Evaluation, Presentation, Interpretation*. New York, Wiley, 352 p.

Rosi, M., L. Vezzoli, P. Aleotti, M. De Censi. 1996. Interaction between caldera collapse and eruptive dyanmics during the Campanian Ignimbrite eruption, Phlegraean Fields, Italy. *Bull. Volcanol*., **57**, 541-554.

Rutherford, M. J., P. M. Hill. 1993. Magma ascent rates from amphibole breakdown: An experimental study applied to the 1980-1986 Mount St. Helens eruption. *J. Geophys. Res*., **98**, 19667-19686.

Swanson, S.E., M.T. Naney, H. R. Westrich, J. C. Eichelberger. 1989. Crystallization history of Obsidian Dome, Inyo Domes, California. *Bull. Volcanol*., **51**, 161-176.

Sylvester, P.J. 1989. Post-collisional alkaline granites. *J. Geol*. **97**, 261-280.

Thieblemont, D., M. Tegyey. 1994. Une discrimination géochimique des roches différenciées témoin de la diversité d'origine et de situation tectonique des magmas calco-alcalins. *C. R. Acad. Sci. Paris*, **319**, II, 87-94.

Tzvetanov, R.G., G.N. Kirov, I.T. Topolova. 1983. Zeolite mineralizations in the tuffs of the Malko-Gradishte and Efrem volcanoes. *Ann. Univ. Sofia, Fac. Geol.- Geogr., 1 – Geol*., **77**, 71-79 (in Bulgarian with an English abstract).

Walker, G.P.L. 1984. Downsag calderas, ring faults, caldera sizes, and incremental caldera growth. *J. Geophys. Res*., **89**, 8407-8416.

Wohletz, K.H., G. Orsi, S. Vita. 1995. Eruptive mechanisms of the Neapolitan Yellow Tuff interpreted from stratigraphy, chemistry, and granulometry. *J. Volcanol. Geotherm. Res*., **67**, 263-290.

Woods, A.W., T. Koyaguchi. 1994. Transition between explosive and effusive eruptions of silicic magmas. *Nature*, **370**, 641-644.

Wright, J.V., G.P.L. Walker. 1977. The ignimbrite source problem: Significance of a co-ignimbrite lag-fall deposit. *Geology*, **5**, 729-732.

Yanev, Y. 1995. General characteristics of the Late Paleogene collision volcanism in the Rhodopes. In: B. Aleksiev (Ed.). *Sofia Zeolite Meeting'95. Intern. Symp.,* Guide Field Trip, 3-19.

Yanev, Y. 1998. Petrology of the Esatern Rhodopes Paleogene acid volcanism, Bulgaria. *Acta Vulcanol*., **10**, 265-277.

Yanev, Y., A. Andreev. 1998. A proposal for classification of the acid volcanics based on the total alkali-silica (TAS) diagram. *C. R. Acad. bulg. Sci*., **53**, 3, 59-62.

Yanev, Y., A. Harkovska., B. Mavrudciev, C. Velcev, P. Nozarov, D. Damjanov. 1975. On the Lozen Palaeogene volcano and its relationship with the deep structure of the Eastern Rhodope Mountains. *Geochem. Mineral. Petrol*., **2**, 90-101 (in Russian with an English abstract).

Yanev, Y., B. Karadjova, A. Andreev. 1983. Distribution of alkalies and genesis of the acid effusives in part of East Rhodope Paleogene depression. *Geol. Balcanica*, **13**, 3, 15-44 (in Russian with an English abstract).

Yanev, Y., F. Innocenti, P. Manetti, G. Serri. 1995. Paleogene collision magmatism in Eastern Rhodopes (Bulgaria) – Western Thrace (Greece): Temporal migration, petro-chemical zoning and geodynamic significance. In: D. Papanikolaou (Ed.). *Proc. 15th Congress of Carpatho-Balkan Geological Association*. Geol. Soc. Greece, Special Publications, **4/2**, 578-583.

Приета на 22.12.2004 г.
Accepted December 22, 2004